Pharmacodynamics of Carbamazepine-mediated Induction of CYP3A4, CYP1A2, and Pgp as Assessed by Probe Substrates Midazolam, Caffeine, and Digoxin

MO Magnusson[1], M-L Dahl[2], J Cederberg[2], MO Karlsson[1] and R Sandström[1]

The aim of this study was to develop a model describing the carbamazepine autoinduction and the carbamazepine-mediated induction of CYP3A4, CYP1A2, and P-glycoprotein. Seven healthy volunteers were dosed with carbamazepine over 16 consecutive days. The CYP3A4, CYP1A2, and P-glycoprotein activities were assessed, using midazolam, caffeine, and digoxin as probe substrates, on 12 occasions, covering the preinduced state and the onset and termination of the induction process. The data were evaluated using a mechanistic pharmacokinetic approach in NONMEM. The induction processes were described using turnover models, with carbamazepine and carbamazepine-10, 11-epoxide as the driving force of the induction. The half-lives of CYP3A4 and CYP1A2 were estimated to be 70 and 105 h, respectively. P-glycoprotein was not affected by the carbamazepine treatment. The possibility of modeling the pharmacodynamics of enzyme induction using a turnover model was illustrated, and the time course of the process was estimated with good precision.

Many drugs enhance the activity of cytochrome *P*450 (CYP) enzymes and thereby change their own metabolism (auto-induction) or the metabolism of other compounds. When assessing induction, the enzyme activity is usually measured before and after a period of treatment with the inducing agent. Thus, the induction magnitude of various CYP enzymes is well known for several inducing agents.[1,2] However, as data are collected only before the start of induction and at the fully induced state, the time course of this process is inadequately described in the literature. To estimate the metabolic capacity at any given point in time during the induction process, the time course of the induction has to be understood.

It has been suggested that a turnover model can be applied to describe the time course of enzyme induction.[3,4] The proposed model consists of a zero-order production rate of enzymes (R_{in}) and a first-order elimination rate constant (k_{out}).[5] An enzyme inducer can increase the amount of enzymes either by increasing the production rate of enzymes or by decreasing the elimination rate. The induction is most often the result of *de novo* protein synthesis,[6] in which case the change in the enzyme amount can be described by equation (1):

$$\frac{dA_{Enzyme}}{dt} = R_{in}S(C(t)) - k_{out}A_{Enzyme} \quad (1)$$

$$k_{out} = \frac{\ln 2}{t_{1/2,\,Enzyme}} \quad (2)$$

where A_{Enzyme} is the amount of enzymes; $C(t)$ describes the pharmacokinetics of the inducer; $S(C(t))$ is the stimulus function, relating the inducer's concentration to the induction stimulus; and $t_{\frac{1}{2},\,Enzyme}$ is the half-life of the enzymes affected by the induction. $t_{\frac{1}{2},\,Enzyme}$ is independent of the characteristics of the inducing compound, making it a system-specific parameter. This parameter is often the main determinant for the time course of the induction process, but the drug-specific stimulus function $S(C(t))$ may also influence the time profile of the induction.

[1]Division of Pharmacokinetics and Drug Therapy, Department of Pharmaceutical Biosciences, Uppsala University, Uppsala, Sweden; [2]Department of Medical Sciences and Clinical Pharmacology, Uppsala University, Uppsala, Sweden. Correspondence: MO Magnusson (Mats.Magnusson@farmbio.uu.se)

Received 28 September 2007; accepted 28 September 2007; advance online publication 31 October 2007. doi:10.1038/sj.clpt.6100431

Certain conditions have to be met to estimate the different parts of the turnover model and to isolate the $t_{\frac{1}{2},\text{Enzyme}}$ parameter: First, an estimation of the amount of a certain CYP isoform requires that the effect of induction is determined using a technique measuring the expression of a specific enzyme. Second, the pharmacokinetics of the inducer have to be described for the establishment of the concentration–stimulus relation. Finally, enzyme activity measurements should be made during both the onset and the cessation of enzyme induction, as, according to the turnover model, the time course of both these processes reflects the half-life of the affected enzyme.

The drugs used in this investigation were carbamazepine, midazolam, caffeine, and digoxin, which have the following characteristics: carbamazepine's most important metabolic pathway is a CYP3A4- and CYP2C8-catalyzed epoxidation to carbamazepine-10,11-epoxide (CBZ-E),[7] which is further metabolized by epoxide hydrolase. Carbamazepine is an inducer of CYP3A4. Moreover, carbamazepine induces CYP1A2 and the efflux protein P-glycoprotein (ABCB1).[8,6] The hydroxylation of midazolam to 1-hydroxymidazolam (1-OH-MDZ) is a marker of CYP3A4 activity;[9] the metabolism of caffeine to paraxanthine is a marker of CYP1A2;[10,11] and the expression of P-glycoprotein can be assessed by digoxin.[12,13]

The aim of this study was to develop a model describing the autoinduction of carbamazepine and the characteristics of the carbamazepine-mediated induction of CYP3A4, CYP1A2, and P-glycoprotein. This was accomplished by dosing seven volunteers with carbamazepine over 16 consecutive days in combination with a cocktail of drugs containing midazolam, caffeine, and digoxin, given before, during, and after the carbamazepine treatment.

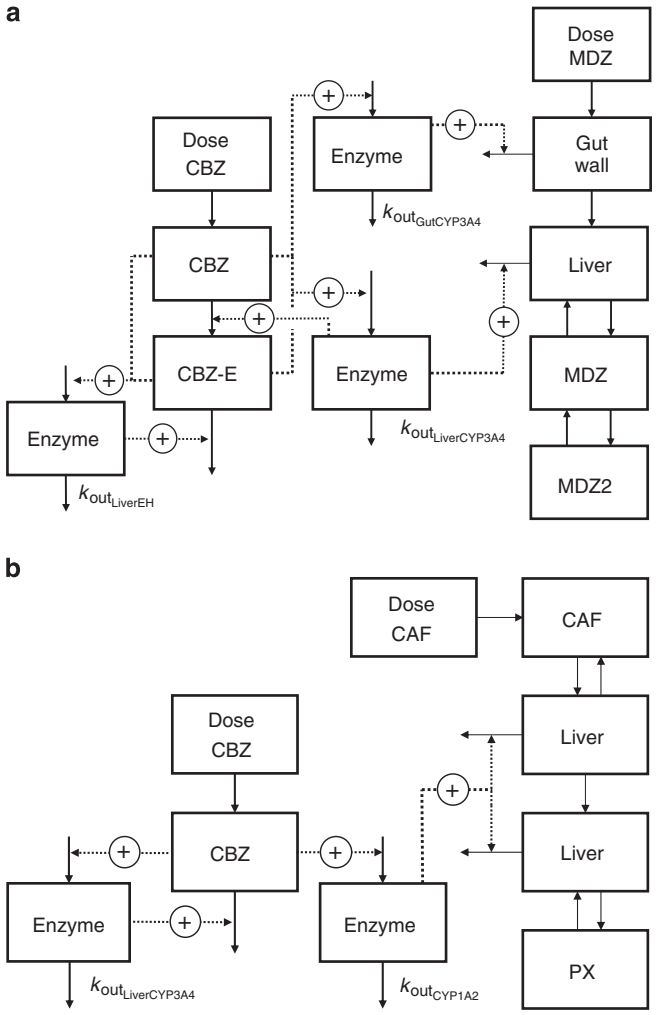

Figure 1 The structure of (**a**) the carbamazepine and midazolam submodels and (**b**) the caffeine submodel. The solid arrows represent flows between compartments. The dashed arrows represent where the amount in a compartment affects the rate constants of another compartment. CBZ, CBZ-E, MDZ, CAF, and PX refer to the compartments associated with carbamazepine, carbamazepine-10,11-epoxide, midazolam, caffeine, and paraxanthine, respectively. k_{out} is the turnover rate constant associated with the different induction processes.

RESULTS

The structure of the final model is presented in Figure 1. All measurements of the carbamazepine, CBZ-E, midazolam, 1-OH-MDZ, 1-OH-MDZ-glucuronide, and digoxin concentrations are presented in Figure 2a. The concentration–time profiles of caffeine and paraxanthine on days 1 and 16 are presented in Figure 2b. The predictive performance of the final model is illustrated in Figure 3. The fixed and random effect parameters obtained from the final model are presented in Table 1 with their corresponding relative standard errors obtained from the bootstraps. The induction magnitudes were linearly correlated with the amount of inducing agents in all models (equation (4)). The time course of all induction processes was described by a turnover model (equation (6)). The individually predicted clearance estimates of carbamazepine, CBZ-E, midazolam, caffeine, and paraxanthine have been plotted vs. time in Figure 4.

Digoxin

The pharmacokinetics of digoxin were described using a two-compartment model. The absorption rate of digoxin changed randomly between different occasions, which was modeled as interoccasion variability rather than a carbamazepine-mediated effect. The carbamazepine treatment did not affect the bioavailability or the elimination rate of digoxin.

Carbamazepine

The final carbamazepine model consisted of one compartment for carbamazepine and one compartment for CBZ-E. The preinduced carbamazepine clearance was 1.3 l/h for a typical individual, increasing to 2.4 l/h after 16 days of induction. The half-life of the carbamazepine autoinduction process was estimated to 69.8 h. The average CBZ-E clearance increased from 5.8 l/h on day 1 to 13.6 l/h on day 16, with an estimated half-life for the CBZ-E induction of 1,180 h. The

bioavailability was fixed to 1 for the administration of 200 mg carbamazepine doses, and the bioavailability of 400 mg doses was estimated to 83%.

Midazolam

A two-compartment model described the pharmacokinetics of midazolam. In addition, a gut wall compartment, allowing a carbamazepine-mediated increase in the extraction ratio across the gut wall mucosa, and a liver compartment, allowing simultaneous changes to occur in the systemic clearance and the first-pass effect, were added. The time course of the carbamazepine-mediated induction was described adequately with two separate turnover models: one for the induction in the gut wall and the other for the induction in the liver metabolism. The half-life of the induction in the gut wall mucosa was fixed to 24 h with a baseline extraction ratio of 43%. The intrinsic clearance of the gut wall ($CL_{int,G}$) increased by 150% in

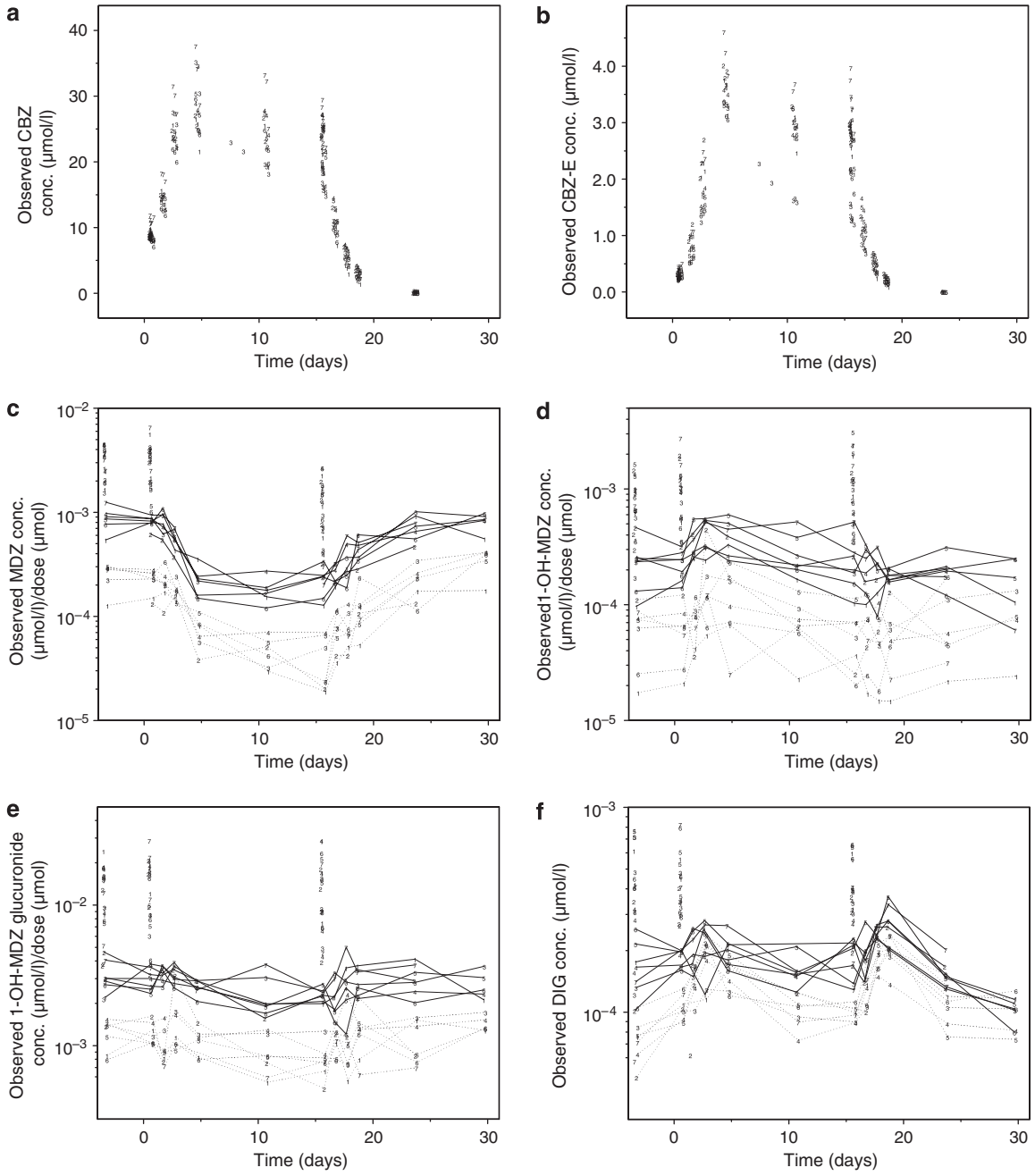

Figure 2 Observed concentrations vs time. (**a**) CBZ, (**b**) CBZ-E, (**c**) MDZ, (**d**) 1-OH-MDZ, (**e**) 1-OH-MDZ-glucuronide, and (**f**) DIG vs. time. The MDZ, 1-OH-MDZ, and 1-OH-MDZ-glucuronide concentrations are dose-adjusted. The numbers represent individual concentrations; the solid and dashed lines connect each individual's 4 and 8 h samples, respectively. (**g**–**j**) Observed concentrations of (**g**) CAF on day 1, (**h**) CAF on day 16, (**i**) PX on day 1, and (**j**) PX on day 16 vs. time. CAF, caffeine; CBZ, carbamazepine; DIG, digoxin; MDZ, midazolam; PX, paraxanthine.

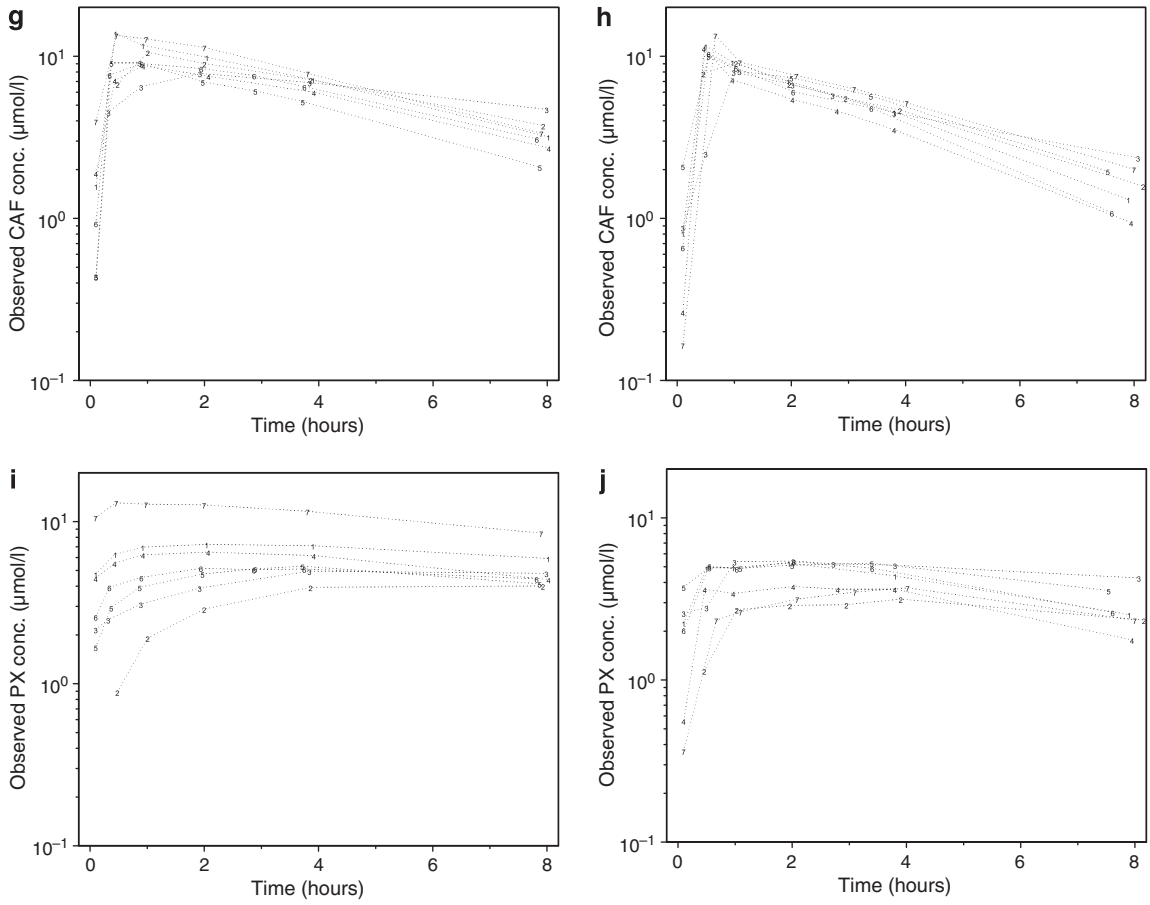

Figure 2 Continued.

the fully induced state, resulting in a gut wall extraction ratio of 66%. The half-life of the liver induction was estimated to be 69.8 h. The initial midazolam clearance was estimated to 38 l/h. The hepatic intrinsic clearance (CL_{int}) had increased by 90% by the end of the carbamazepine treatment period, which resulted in a clearance of 54 l/h.

The 1-OH-MDZ concentrations increased untill day 5, but decreased by days 11 and 16. No trends were observed in the 1-OH-MDZ-glucuronide concentrations.

Caffeine

The caffeine model consisted of one sampling compartment and one liver compartment for caffeine and paraxanthine, respectively. The caffeine CL_{int} increased by 27% at the fully induced state, resulting in a change in clearance from 8.4 to 10.4 l/h. The paraxanthine CL_{int} increased by 47% in response to the carbamazepine treatment, resulting in an increased clearance from 6.9 to 9.9 l/h. The half-life of the induction process was estimated to be 105 h.

Genotyping

No variant alleles of CYP3A4 were found among the subjects. All were homozygous for Cyp3a5*3, indicating lack of expression of CYP3A5.

DISCUSSION

The pharmacokinetics of carbamazepine, CBZ-E, midazolam, caffeine, and paraxanthine changed as a result of the carbamazepine treatment. The time-dependent pharmacokinetics were described with a model where the production rates of the affected enzymes were proportional to the amounts of the inducing agents (equation (4)), and the time course of the induction process was described by the turnover model (equation (6)). Previous *in vitro* experiments[14] show a saturable concentration–induction magnitude relation, which can be described by the E_{max} function (equation (5)), and a negative correlation between baseline enzyme activity and the induction magnitude, suggesting a maximal synthesis rate of the proteins. In this investigation, a linear relation between the inducers and the stimulus was sufficient to describe the data, and the model was not further improved by using an E_{max} function, probably owing to the narrow carbamazepine dose range used in this investigation. It is possible that a more potent inducer or higher doses of carbamazepine could result in a nonlinear relation. The evaluated stimulus functions are of course empirical ways to describe the concentration–response relation. However, a truly mechanistic model requires knowledge about the unbound concentration of the inducer inside the liver cell, the number

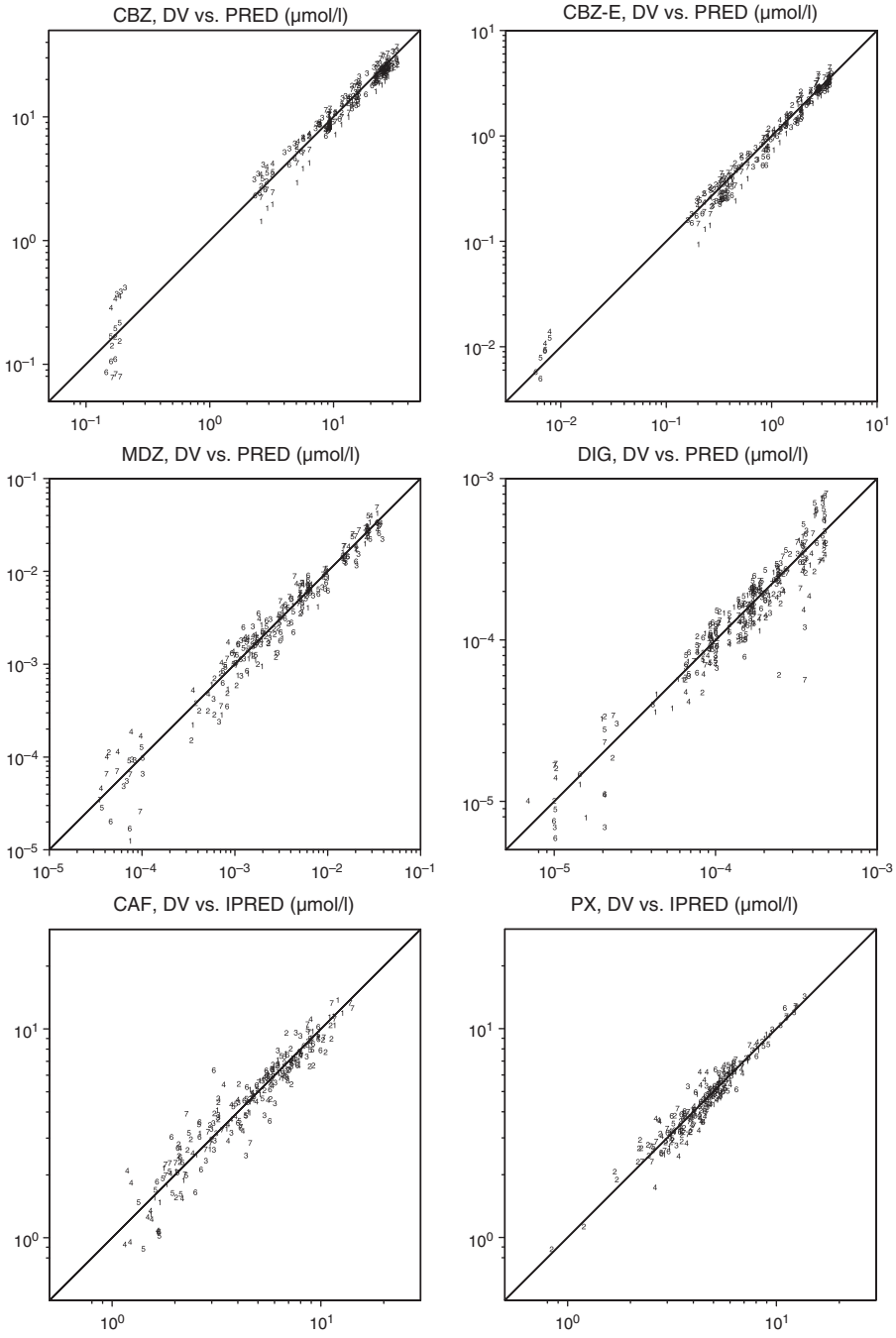

Figure 3 Observed concentrations (DV) vs. predicted concentrations (PRED) for CBZ, CBZ-E, MDZ, and DIG. Observed concentrations vs. individual predicted concentrations (IPRED) for CAF and PX. CAF, caffeine; CBZ, carbamazepine; DIG, digoxin; MDZ, midazolam; PX, paraxanthine.

of nuclear receptors, the binding affinity between nuclear receptors and DNA, the mRNA production rate, and the rate with which mRNA is turned into a CYP enzyme. Many of these parameters are not easily obtained with current techniques, and an empirical approach was therefore used in this part of the model.

Previous studies have suggested a shorter half-life for the onset of the induction than for its cessation,[15,16] which is not anticipated by the turnover model. However, the plasma concentrations of the inducing agent were not measured in these former studies. If the terminal half-life of the compound causing the induction is of the same magnitude as the half-life of the induced enzymes, the kinetics of the inducing agent will affect the apparent half-life of the induction process.[17] In this investigation, the preinduced half-life of carbamazepine was 40 h, and the half-lives of the induction of CYP3A4 and CYP1A2 were 70 and 105 h, respectively. When a step model (equation (3)) was applied to the stimulus function, our model also estimated a shorter half-life of the enzyme during the onset of the induction than

Table 1 Parameter estimates with corresponding relative standard errors

Parameter	Estimate	RSE (%)	Inter individual variability (%)	RSE (%)
Carbamazepine[a]				
CL/*F* CBZ→CBZ-E (l/h)	0.253	7.4	16.9	44
CL/*F* total baseline (l/h)	1.27	—	—	—
V/*F* (l)	73.4	4.2	11.8	53
k_a (h^{-1})	0.2 (fix)	—	—	—
Induction slope CL_{CBZ} (%IND per μg CBZ+CBZ-E)	0.22	15.3	33.0	43
$t_{1/2}$ CBZ induction (h)	69.7	8.7	—	—
F 400 mg CBZ (%)	83	2.5	—	—
Prop. residual error CBZ (%)	6.64	10.1	—	—
CBZ-E[a]				
CL (l/h)	5.82	10.7	12.8	61
V (l)	36.3	25.0	56.6	135
Induction slope CL_{CBZ-E} (%IND per mg CBZ+CBZ-E)	0.39	79	—	—
$t_{1/2}$ CBZ-E induction (h)	1,180	75	—	—
Prop. residual error CBZ-E (%)	9.14	12.9	—	—
Midazolam[b]				
CL hepatic, baseline (l/h)	38.9	3.3	6.2	58
V_1 (l)	84.4	5.2	—	—
V_2 (l)	41.4	25.3	16.1	56
Q (l/h)	9.24	22.6	12.	88
k_a (h^{-1})	1.81	—	—	—
Induction slope hepatic induction (%IND per μg CBZ+CBZ-E)	0.0462	19.5	5.1	60
$t_{1/2}$ hepatic induction (h)	69.7	8.9	—	—
Gut wall extraction ratio (%)	43 (fix)	—	—	—
Induction slope gut wall extr. (%IND/μg CBZ+CBZ-E)	0.0847	31.5	—	—
$t_{1/2}$ gut wall induction (h)	24 (fix)	—	—	—
Prop. residual error (%)	28.0	11.1	—	—
Digoxin[a]				
CL (l/h)	29.1	4.2	10	40
V_1 (l)	175	16	45	48
V_2 (l)	1,060	7.2	15	48
Q (l/h)	111	6.2	—	—
k_a (h^{-1})	1.43	9.0	—	—
IOV k_a (%)	53	44	—	—
Prop. residual error (%)	21.7	7.6	—	—
Additive residual error (nmol/l)	0.0051	20	—	—
Caffeine[b]				
CL (l/h)	8.35	5.3	16	45
V (l)	41.7	6.8	14	45
k_a (h^{-1})	4.24	—	—	—
IOV k_a (%)	125	—	—	—
Induction slope CL (%IND per μg CBZ+CBZ-E)	0.0162	23	24	143
$t_{1/2}$ induction (h)	105	22	—	—
Paraxanthine[b]				
CL (l/h)	6.84	4.1	11	96
V (l)	32.9	3.1	—	—
Induction slope CL (%IND per μg CBZ+CBZ-E)	0.0272	17	32	115
$t_{1/2}$ induction (h)	105	22	—	—

CBZ, carbamazepine; CBZ-E, carbamazepine-10,11-epoxide; CL, clearance; F, bioavailability; IND, induction; IOV, interoccasion variability; k_a, absorption rate constant; prop. residual error, proportional residual error; *Q*, intercompartmental clearance; RSE, relative standard error; $t_{1/2}$ induction, half-life of the induction; *V* and V_1, volume of sampling compartment; V_2, volume of peripheral compartment. [a]Modeling performed on plasma concentrations. [b]Modeling performed on blood concentrations.

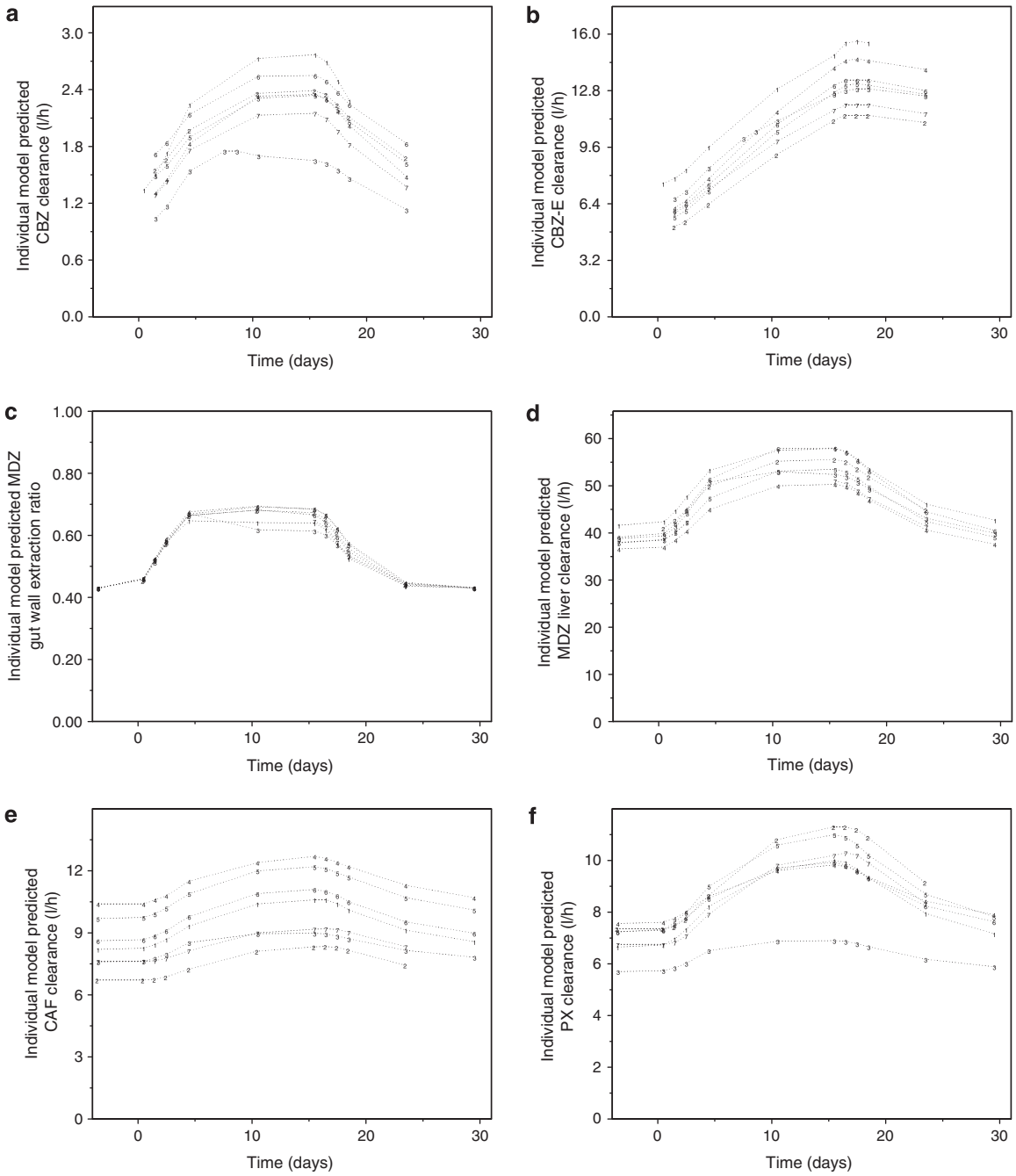

Figure 4 Individual predicted clearance of (**a**) CBZ, (**b**) CBZ-E, (**d**) MDZ, (**e**) CAF, and (**f**) PX vs. time. (**c**) Individual predicted gut wall extraction ratio of MDZ vs. time. CAF, caffeine; CBZ, carbamazepine; MDZ, midazolam; PX, paraxanthine.

for its cessation. However, a symmetrical model was obtained; *i.e.*, the k_{out} was estimated to be the same during the initiation of the induction as when the enzyme activity declined, by including the pharmacokinetics of the inducer in the model.

All pharmacodynamic models described in equations (3–6) were evaluated for the induction of elimination of each compound. In addition, effects of the inducer on the turnover rate of the enzymes were examined. A linear stimulus function affecting the production rate of the enzyme turned out to be the best model for all compounds. Both the amount and the concentration of the inducers in the central compartments were evaluated as being the driving force of the induction. These two approaches did not differ significantly, but to avoid the possibility for the model to explain a reduced induction magnitude by increasing the volume of distribution, the amounts were preferred to the concentrations in the final model. Competitive inhibition

between carbamazepine and the probe compounds is unlikely, as the pharmacokinetics of the probe compounds did not change significantly from day −3 to day 1.

The absence of a carbamazepine-mediated effect on the pharmacokinetics of digoxin was surprising, as it has been suggested that P-glycoprotein can be induced by carbamazepine.[6] However, a recent study reported that carbamazepine does not alter P-glycoprotein expression.[18]

The increase in the carbamazepine plasma concentration on day 3 (first 400 mg dose of carbamazepine) was less than expected. The reason for this could be either a very rapid induction process (*e.g.*, owing to induction in gut wall metabolism) or the result of dose-dependent bioavailability. A peroral solution of carbamazepine has complete bioavailability, and therefore, a gut wall metabolism is unlikely.[19] However, dose-dependent pharmacokinetics of carbamazepine have been reported,[20] which could be the result of poor solubility. Therefore, the bioavailability of 200 mg carbamazepine dose was fixed to 1, whereas the bioavailability of 400 mg dose was estimated to be 83%.

The CBZ-E clearance was doubled on day 16, which is in agreement with reported carbamazepine-mediated changes in CBZ-E metabolism.[21] The half-life of the induction of the metabolism of CBZ-E was estimated to be 1,180 h. However, the CBZ-E pharmacokinetic parameters are correlated to the fraction of carbamazepine being metabolized into this metabolite. The half-life of the CBZ-E induction process should therefore be viewed with great skepticism, as it is dependent on the inducibility of carbamazepine's metabolic pathways.

The structure of the midazolam model, including a liver compartment, allowed a change in the hepatic metabolic clearance to simultaneously affect the bioavailability and systemic clearance of midazolam. However, by day 16, the level of induction in the systemic midazolam clearance was too low to explain fully the decreased midazolam exposure. CYP3A4 is the most abundant CYP enzyme in the gut wall mucosa,[22] and midazolam is extensively metabolized when it is absorbed.[23] Induction in the extraction ratio over the gut wall affects the bioavailability of a drug without changing the systemic elimination. To explain the more pronounced change in the bioavailability than in the systemic clearance, it was assumed that induction also affected the gut wall extraction ratio. However, the half-life of the gut wall induction could not be determined with the applied study design, so the half-life of the gut wall epithelium was assumed to be the rate-limiting step for this process and was fixed to 24 h as reported.[24–26] To separate enzyme induction in the gut wall from the liver, a more advanced protocol is required, with more intensive dosing and sampling during the first days following the induction onset. Also, the probe compound has to be simultaneously dosed intravenously and perorally (labeled compound). Moreover, it would not be possible to stagger the dosing of carbamazepine and the probe, which could lead to interactions during the absorption phase. The estimated systemic half-life of CYP3A4 of 70 h is in agreement with the turnover rate of CYP3A4 reported in other studies (see review by Ghanbari *et al.*[27]). It cannot be ruled out that carbamazepine might have increased the plasma protein levels, which could have resulted in a downward bias in the midazolam induction magnitude estimate.

The ratio of the plasma concentrations of 1-OH-MDZ and midazolam is commonly used as a marker for CYP3A4 activity, and therefore, the 1-OH-MDZ concentration measurements were expected to contribute to the midazolam model. But, although the 1-OH-MDZ concentrations increased during the first 5 days of carbamazepine treatment, from day 11 onward, the 1-OH-MDZ concentrations decreased. An attempt was made to include the 1-OH-MDZ and the 1-OH-MDZ-glucuronide concentrations in the model, but this did not improve the understanding of midazolam pharmacokinetics or the time course of the CYP3A4 induction process, so these data were excluded during the modeling process. In a recent report, the midazolam clearance was found to be a good measurement for CYP3A4 activity; however, the 1-OH-MDZ/midazolam concentration ratio could not at any point in time accurately predict the midazolam clearance.[28]

Consumption of caffeine was permitted between the sampling days. Therefore, the trough plasma samples withdrawn before administration of the cocktail of drugs contained caffeine and paraxanthine, but without a valid caffeine dosing record. This was handled by estimating the trough concentrations of caffeine and paraxanthine on each occasion, which required extensive use of interoccasion variability parameters, and as a consequence, it took about a month for each model to converge. The run times were reduced to less than a week when the contribution of CBZ-E to the induction magnitude was excluded and the inter-individual variability was fixed to 0 in the carbamazepine kinetic submodel. The exclusion of the contribution of CBZ-E to the induction of caffeine and paraxanthine probably had a limited impact on the model, as the CBZ-E concentrations were only one-tenth of the carbamazepine concentrations. It was quite surprising that paraxanthine elimination was induced more strongly than caffeine elimination, as both compounds are metabolized by CYP1A2.[29] However, other enzymes are involved in the metabolism of these compounds, and the differences in CYP isoforms involved in these alternative metabolic routes could explain the difference in the induction magnitude.

In summary, the possibility to model the pharmacodynamics of enzyme induction using a turnover model has been illustrated here. Symmetrical induction models, with the same half-life of the induced enzymes during the onset of induction and during its cessation, were obtained by including the pharmacokinetic and pharmacodynamic relations in the model. The half-life of the induction in hepatic CYP3A4 was estimated to be 70 h and the induction of CYP1A2 had a half-life of 105 h. This information can be of great value when designing interaction experiments and also

when making adjustments in doses after the initialization or termination of treatment with enzyme-inducing compounds. To the best of our knowledge, this is the first model describing the pharmacodynamics of enzyme induction for specific CYP enzymes in a controlled clinical trial.

METHODS

Subjects. Seven healthy volunteers were enrolled in the study after passing a health screen imposing the following inclusion criteria: non-smoking, male, Caucasian, 20–45 years, and declared healthy after physical examination. The subjects abstained from drugs, alcohol, and grapefruit juice during the study, and from caffeine-containing beverages during the sampling days. Written informed consents were obtained before inclusion. The study was approved by the ethics committee of Uppsala University and by the Swedish Medical Products Agency, and was conducted in accordance with the Declaration of Helsinki Principles.

Study design. Subjects enrolled in the study received daily doses of 200 mg carbamazepine for 2 days, followed by 400 mg carbamazepine for 14 days. Subject 3 reported nausea on day 5, so the carbamazepine was reduced to 200 mg for this individual. All doses were administered once per day at 2000 hours. The various days on which the study took place are referred to as day −3 to 30, where day 0 is the day of the first carbamazepine dose. A peroral drug cocktail containing 2.5 or 5.0 mg midazolam, 100 mg caffeine, and 0.13 mg digoxin was administered at 0800 hours on days −3, 1, 2, 3, 5, 11, 16, 17, 18, 19, 24, and 30. Extensive CYP3A4 induction could lead to unquantifiable plasma concentrations of midazolam. The midazolam concentrations were therefore monitored during the investigation, and the dose was increased to 5.0 mg on days 5–18 for subjects 1, 3, and 4, and on days 11–18 for subjects 5, 6, and 7.

Drugs. Carbamazepine 200 and 400 mg tablets (Tegretol; Novartis, Täby, Sweden), midazolam 1 mg/ml oral solution (APL, Stockholm, Sweden), caffeine 100 mg tablets (Koffein Recip; Recip, Årsta, Sweden), and digoxin 0.13 mg tablets (Lanacrist; AstraZeneca, Södertälje, Sweden) were all purchased from Apoteket AB (Stockholm, Sweden).

Blood sampling. Venous blood samples were collected into Li-heparin Vacutainer tubes (Becton-Dickinson, Franklin Lakes, NJ) by vein puncture in the arm 5 min before the cocktail of drugs was given and 4 and 8 h after the dose. In addition, blood samples were collected 0.5, 1, and 2 h after the cocktail was given on days −3, 1, and 16. Each sample was centrifuged for 10 min followed by immediate separation of the plasma, which was stored at −20°C awaiting chemical analysis.

Chemical analysis. The plasma concentrations of midazolam, 1-OH-MDZ, caffeine, and paraxanthine were measured by HPLC–MS/MS (high-performance liquid chromatography–tandem mass spectrometry) before and after an incubation with β-glucuronidase, as described by Scott *et al.*[10] This method was modified to include carbamazepine and CBZ-E. The digoxin plasma concentrations were measured in accordance with Yao *et al.*[30] The sample preparation and the analytical system setup were identical to the work by Asimus *et al.*[31] The 1-OH-MDZ-glucuronide concentrations were calculated as the difference between 1-OH-MDZ concentrations before and after incubation with β-glucuronidase.

Genotyping. DNA was isolated from peripheral leukocytes by the QIAamp DNA Blood Mini Kit (Qiagen, Hilden, Germany), according to the guidelines of the manufacturer. *CYP3A4*1B*, *CYP3A4*3*, and *CYP3A4*4*, as well as *CYP3A5*2* and *CYP3A5*6* alleles were analyzed by allele-specific PCR followed by digestion with restriction enzymes.[32–35] *CYP3A5*3* allele was analyzed by TaqMan allelic discrimination in the ABI PRISM 7000 Sequence Detection System.[36]

Data analysis. The model that best describes the pharmacokinetics of the investigated compounds and the pharmacodynamics of enzyme induction was determined through nonlinear mixed-effect modeling using the first-order conditional estimation method in NONMEM, version VIβ.[37] The estimated population model parameters were the fixed-effect parameters, related to the typical individual, and the random-effect parameters, describing the magnitudes of interindividual variability in parameters (log-normally distributed) and residual variability between individual predictions and observations (constant and/or proportional error models). The difference in the value of the objective function (−2 log-likelihood) produced by NONMEM is a standard tool to discriminate between two nested models. A drop in the objective function value of >3.84 per parameter included is usually regarded as a statistically significant improvement ($P<0.05$). However, the value of the objective function corresponding to $P<0.05$ is higher than 3.84 for data sets with few individuals,[38] so a drop in the objective function value of 10 was regarded as statistically significant in this work. The model-building process was guided by graphical evaluations using S-Plus (Insightful, Seattle, WA), with the Xpose library.[39] The NONMEM-generated standard errors of the final model's parameters were confirmed by 200 sample bootstraps for the digoxin, carbamazepine, and midazolam submodels, and 60 sample bootstraps for the caffeine submodel (because of long run times). The bootstraps were performed by resampling on the individual level using the PsN toolkit.[40]

The model was developed on log-transformed data using a sequential approach as follows: First, a pharmacokinetic submodel, including autoinduction, was developed for carbamazepine and CBZ-E. Then, the parameters from the carbamazepine submodel were fixed to their final estimates, and the carbamazepine data set was merged with the data sets of midazolam, caffeine, and digoxin, thereby forming three new data sets. The carbamazepine submodel was used as the driving force for enzyme induction in development of the other compound's submodels.

Modeling the pharmacodynamics of induction. The induction potential of CBZ-E has been reported to be similar to that of carbamazepine.[18] Therefore, the total amounts of carbamazepine and CBZ-E affect the induction magnitude. The following stimulus functions were evaluated for all compounds: a step model (equation (3)), a linear model (equation (4)), and a nonlinear model (equation (5)):

$$\text{induction} = \text{IND}_{\text{Max}}\,\text{CBZ}_{1/0} \tag{3}$$

$$\text{induction} = \text{IND}_{\text{Slope}}\,A_{\text{CBZ}} \tag{4}$$

$$\text{induction} = \frac{\text{IND}_{\text{Max}}\,A_{\text{CBZ}}}{K_{\text{m,induction}} + A_{\text{CBZ}}} \tag{5}$$

where IND_{Max} is the maximal induction, $\text{CBZ}_{1/0}$ is 1 or 0, depending on the presence of the inducer, A_{CBZ} is the amount of inducers, $\text{IND}_{\text{Slope}}$ is relating A_{CBZ} to the induction magnitude, and $K_{\text{m,induction}}$ is the amount of inducers corresponding to half maximal induction.

The time course of the induction was described by a turnover model:

$$\frac{dA_{\text{Enzyme}}}{dt} = R_{\text{in}}(1 + \text{induction}) - k_{\text{out}}A_{\text{Enzyme}} \tag{6}$$

where R_{in} is the zero-order production rate, k_{out} is the first-order turnover rate constant, and A_{Enzyme} is the enzyme amount. A_{Enzyme}

was normalized to 1 in the preinduced state by setting R_{in} equal to k_{out}. The efficacy of the eliminating organ (CL_{int}) was assumed to be proportional to A_{Enzyme}. The time course of the hepatic induction was initially estimated using separate parameters for the induction of the elimination of carbamazepine, CBZ-E, midazolam, caffeine, and paraxanthine. However, similar estimates were obtained for the parameters for the time course of carbamazepine autoinduction and midazolam induction. CYP3A4 is known to contribute to carbamazepine autoinduction and is the main midazolam-metabolizing enzyme, So in the final model, these two processes were assumed to have the same k_{out} (k_{out} being the only unfixed carbamazepine parameter in the final model). Caffeine and paraxanthine are both metabolized by CYP1A2, and their induction processes were therefore assumed to have the same k_{out}.

Digoxin. The pharmacokinetics of digoxin were evaluated with first-order absorption and a linear elimination model, parameterized in terms of clearance and the volume of distribution. The effect of carbamazepine-mediated induction on the absorption rate, bioavailability, and the elimination rate of digoxin was evaluated by using equations (3–5).

Carbamazepine. The pharmacokinetics of carbamazepine and CBZ-E were described by a model with first-order absorption and a linear elimination model. The fraction of carbamazepine being metabolized to CBZ-E has been reported to be 20% after a single carbamazepine dose, but increases with the number of doses owing to enzyme induction.[41] Therefore, two carbamazepine clearances describe the elimination of carbamazepine, an inducible clearance (CL_{CBZ1}), assumed to form CBZ-E, and an uninducible clearance (CL_{CBZ2}), forming unmeasured metabolites. CL_{CBZ2} was fixed to four times CL_{CBZ1} before induction.

Midazolam. Midazolam is metabolized in the gut wall mucosa before entering the liver,[23] so the midazolam extraction ratio over the gut wall (E_G) was estimated using a model developed by Yang *et al.*:[42]

$$F_G = 1 - E_G = 1 - \frac{CL_{int,G}\, f_{u,G}}{Q_G + CL_{int,G}\, f_{u,G}} \quad (7)$$

where $CL_{int,G}$ is the intrinsic clearance of the gut wall, $f_{u,G}$ is the unbound fraction in the gut wall, fixed to 1, and Q_G is the rate of drug diffusion over the gut wall mucosa, also fixed to 1. The midazolam gut wall extraction ratio was fixed to 43% before induction.[23] The inducibility of the intrinsic clearance of the gut wall was evaluated with the induction models in equations (3–5). The time course of the gut wall induction process was described by using the turnover model in equation (6), with the half-life of the induction process fixed to 24 h.[24–26]

A liver compartment was inserted between the gut wall and the sampling compartments, allowing the development of a semi-physiological model as described in detail by Gordi *et al.*,[43] with a hepatic extraction ratio and clearance described by the well-stirred model:

$$E_H = \frac{CL_{int}\, f_u}{Q_H + CL_{int}\, f_u} \quad (8)$$

$$CL_H = Q_H E_H \quad (9)$$

$$F_H = 1 - E_H \quad (10)$$

where E_H represents the extraction ratio across the liver, f_u is the unbound fraction, Q_H is the blood flow to the liver, and F_H is the hepatic bioavailability; f_u was 3.5%,[44] the blood–plasma concentration ratio was 0.7,[45] and the blood flow was 100 l/h.[46] The midazolam concentrations were transformed to blood concentrations and f_u was transformed to its equivalent f_u in blood. General equations for the distribution and elimination of compounds in the liver and in the sampling compartments are presented in the following equations:

$$\frac{dA_H}{dt} = k_a A_1 F_G - Q_H C_H \quad (11)$$

$$\frac{dA_S}{dt} = F_H Q_H A_H - k_{SH} A_S \quad (12)$$

$$k_{SH} = \frac{Q_H}{V_S} \quad (13)$$

where A_1, A_H, and A_S are the amounts of the compound in the dosing compartment, the liver compartment, and the sampling compartment, respectively; C_H is the concentration of the drug in the liver compartment; k_{SH} is the rate constant by which the drug is transported to the liver from the sampling compartment; and V_S is the volume of the sampling compartment, assumed to be 1 l.

Caffeine. A semi-physiological model describing the caffeine and paraxanthine data, similar to that adopted by the midazolam submodel was developed. The unbound fraction was assumed to be 0.68 for caffeine and 0.54 for paraxanthine, with a blood–plasma concentration ratio of 1.[47] The fraction of caffeine metabolized to paraxanthine was fixed to 84%.[48] The trough caffeine and paraxanthine concentrations were estimated on each occasion, similar to the "missing dose method" described by Soy *et al.*[49] Interoccasion variability in the absorption rate was applied to the caffeine absorption on days −3, 1, and 16. The complexity of the model led to problems associated with the time required for the model to converge. To address this, the model was simplified by removing CBZ-E contribution to the induction of caffeine and paraxanthine metabolism and by excluding all interindividual variability in the pharmacokinetics of carbamazepine.

ACKNOWLEDGMENTS

We are grateful to Inga-Lena Sporrong, Britt Jansson, Siv Jönsson, Lars Lindbom, and Maria Gabriella Scordo for valuable contributions to this work.

CONFLICT OF INTEREST

The authors declared no conflict of interest.

1. Yeh, R.F. *et al.* Lopinavir/ritonavir induces the hepatic activity of cytochrome *P*450 enzymes CYP2C9, CYP2C19, and CYP1A2 but inhibits the hepatic and intestinal activity of CYP3A as measured by a phenotyping drug cocktail in healthy volunteers. *J. Acquir. Immune Defic. Syndr.* **42,** 52–60 (2006).
2. Branch, R.A., Adedoyin, A., Frye, R.F., Wilson, J.W. & Romkes, M. *In vivo* modulation of CYP enzymes by quinidine and rifampin. *Clin. Pharmacol. Ther.* **68,** 401–411 (2000).
3. Levy, R.H., Lai, A.A. & Dumain, M.S. Time-dependent kinetics IV: pharmacokinetic theory of enzyme induction. *J. Pharm. Sci.* **68,** 398–399 (1979).
4. Garlick, P.J., Waterlow, J.C. & Swick, R.W. Measurement of protein turnover in rat liver. Analysis of the complex curve for decay of label in a mixture of proteins. *Biochem. J.* **156,** 657–663 (1976).
5. Dayneka, N.L., Garg, V. & Jusko, W.J. Comparison of four basic models of indirect pharmacodynamic responses. *J. Pharmacokinet. Biopharm.* **21,** 457–478 (1993).
6. Giessmann, T. *et al.* Carbamazepine regulates intestinal P-glycoprotein and multidrug resistance protein MRP2 and influences disposition of talinolol in humans. *Clin. Pharmacol. Ther.* **76,** 192–200 (2004).

7. Kerr, B.M. *et al.* Human liver carbamazepine metabolism. Role of CYP3A4 and CYP2C8 in 10,11-epoxide formation. *Biochem. Pharmacol.* **47,** 1969–1979 (1994).
8. Parker, A.C., Pritchard, P., Preston, T. & Choonara, I. Induction of CYP1A2 activity by carbamazepine in children using the caffeine breath test. *Br. J. Clin. Pharmacol.* **45,** 176–178 (1998).
9. Thummel, K.E. *et al.* Use of midazolam as a human cytochrome *P*450 3A probe: I. *In vitro–in vivo* correlations in liver transplant patients. *J. Pharmacol. Exp. Ther.* **271,** 549–556 (1994).
10. Scott, R.J., Palmer, J., Lewis, I.A. & Pleasance, S. Determination of a ''GW cocktail'' of cytochrome *P*450 probe substrates and their metabolites in plasma and urine using automated solid phase extraction and fast gradient liquid chromatography tandem mass spectrometry. *Rapid Commun. Mass Spectrom.* **13,** 2305–2319 (1999).
11. Christensen, M. *et al.* The Karolinska cocktail for phenotyping of five human cytochrome *P*450 enzymes. *Clin. Pharmacol. Ther.* **73,** 517–528 (2003).
12. Greiner, B. *et al.* The role of intestinal P-glycoprotein in the interaction of digoxin and rifampin. *J. Clin. Invest.* **104,** 147–153 (1999).
13. Drescher, S., Glaeser, H., Murdter, T., Hitzl, M., Eichelbaum, M. & Fromm, M.F. P-glycoprotein-mediated intestinal and biliary digoxin transport in humans. *Clin. Pharmacol. Ther.* **73,** 223–231 (2003).
14. Kostrubsky, V.E. *et al.* The use of human hepatocyte cultures to study the induction of cytochrome *P*-450. *Drug Metab. Dispos.* **27,** 887–894 (1999).
15. von Bahr, C., Steiner, E., Koike, Y. & Gabrielsson, J. Time course of enzyme induction in humans: effect of pentobarbital on nortriptyline metabolism. *Clin. Pharmacol. Ther.* **64,** 18–26 (1998).
16. Fromm, M.F., Busse, D., Kroemer, H.K. & Eichelbaum, M. Differential induction of prehepatic and hepatic metabolism of verapamil by rifampin. *Hepatology* **24,** 796–801 (1996).
17. Abramson, F.P. Kinetic models of induction: I. Persistence of the inducing substance. *J. Pharm. Sci.* **75,** 223–228 (1986).
18. Oscarson, M., Zanger, U.M., Rifki, O.F., Klein, K., Eichelbaum, M. & Meyer, U.A. Transcriptional profiling of genes induced in the livers of patients treated with carbamazepine. *Clin. Pharmacol. Ther.* **80,** 440–456, e7 (2006).
19. Gerardin, A., Dubois, J.P., Moppert, J. & Geller, L. Absolute bioavailability of carbamazepine after oral administration of a 2% syrup. *Epilepsia* **31,** 334–338 (1990).
20. Kumps, A.H. Dose-dependency of the ratio between carbamazepine serum level and dosage in patients with epilepsy. *Ther. Drug Monit.* **3,** 271–274 (1981).
21. Eichelbaum, M., Tomson, T., Tybring, G. & Bertilsson, L. Carbamazepine metabolism in man. Induction and pharmacogenetic aspects. *Clin. Pharmacokinet.* **10,** 80–90 (1985).
22. Paine, M.F., Hart, H.L., Ludington, S.S., Haining, R.L., Rettie, A.E. & Zeldin, D.C. The human intestinal cytochrome *P*450 ''pie''. *Drug Metab. Dispos.* **34,** 880–886 (2006).
23. Thummel, K.E. *et al.* Oral first-pass elimination of midazolam involves both gastrointestinal and hepatic CYP3A-mediated metabolism. *Clin. Pharmacol. Ther.* **59,** 491–502 (1996).
24. Nakshabendi, I.M., McKee, R., Downie, S., Russell, R.I. & Rennie, M.J. Rates of small intestinal mucosal protein synthesis in human jejunum and ileum. *Am. J. Physiol.* **277,** E1028–E1031 (1999).
25. Greenblatt, D.J. *et al.* Time course of recovery of cytochrome *p*450 3A function after single doses of grapefruit juice. *Clin. Pharmacol. Ther.* **74,** 121–129 (2003).
26. Takanaga, H. *et al.* Relationship between time after intake of grapefruit juice and the effect on pharmacokinetics and pharmacodynamics of nisoldipine in healthy subjects. *Clin. Pharmacol. Ther.* **67,** 201–214 (2000).
27. Ghanbari, F. *et al.* A critical evaluation of the experimental design of studies of mechanism based enzyme inhibition, with implications for *in vitro–in vivo* extrapolation. *Curr. Drug Metab.* **7,** 315–334 (2006).
28. Lee, L.S., Bertino, J.S. Jr. & Nafziger, A.N. Limited sampling models for oral midazolam: midazolam plasma concentrations, not the ratio of 1-hydroxymidazolam to midazolam plasma concentrations, accurately predicts AUC as a biomarker of CYP3A activity. *J. Clin. Pharmacol.* **46,** 229–234 (2006).
29. Kalow, W. & Tang, B.K. The use of caffeine for enzyme assays: a critical appraisal. *Clin. Pharmacol. Ther.* **53,** 503–514 (1993).
30. Yao, M., Zhang, H., Chong, S., Zhu, M. & Morrison, R.A. A rapid and sensitive LC/MS/MS assay for quantitative determination of digoxin in rat plasma. *J. Pharm. Biomed. Anal.* **32,** 1189–1197 (2003).
31. Asimus, S. *et al.* Artemisinin antimalarials moderately affect cytochrome *P*450 enzyme activity in healthy subjects. *Fundam. Clin. Pharmacol.* **21,** 307–316 (2007).
32. van Schaik, R.H., de Wildt, S.N., Brosens, R., van Fessem, M., van den Anker, J.N. & Lindemans, J. The CYP3A4*3 allele: is it really rare? *Clin. Chem.* **47,** 1104–1106 (2001).
33. van Schaik, R.H., de Wildt, S.N., van Iperen, N.M., Uitterlinden, A.G., van den Anker, J.N. & Lindemans, J. CYP3A4-V polymorphism detection by PCR-restriction fragment length polymorphism analysis and its allelic frequency among 199 Dutch Caucasians. *Clin. Chem.* **46,** 1834–1836 (2000).
34. van Schaik, R.H., van der Heiden, I.P., van den Anker, J.N. & Lindemans, J. CYP3A5 variant allele frequencies in Dutch Caucasians. *Clin. Chem.* **48,** 1668–1671 (2002).
35. Wang, A. *et al.* Ile118Val genetic polymorphism of CYP3A4 and its effects on lipid-lowering efficacy of simvastatin in Chinese hyperlipidemic patients. *Eur. J. Clin. Pharmacol.* **60,** 843–848 (2005).
36. Mirghani, R.A. *et al.* CYP3A5 genotype has significant effect on quinine 3-hydroxylation in Tanzanians, who have lower total CYP3A activity than a Swedish population. *Pharmacogenet. Genomics* **16,** 637–645 (2006).
37. Beal, S.L. & Sheiner, L.S. *NONMEM User's Guides* (GloboMax, Hanover, MD, 1989–1998).
38. Wahlby, U., Jonsson, E.N. & Karlsson, M.O. Assessment of actual significance levels for covariate effects in NONMEM. *J. Pharmacokinet. Pharmacodyn.* **28,** 231–252 (2001).
39. Jonsson, E.N. & Karlsson, M.O. Xpose—an S-PLUS based population pharmacokinetic/pharmacodynamic model building aid for NONMEM. *Comput. Methods Programs Biomed.* **58,** 51–64 (1999).
40. Lindbom, L., Pihlgren, P. & Jonsson, E.N. PsN-Toolkit—a collection of computer intensive statistical methods for non-linear mixed effect modeling using NONMEM. *Comput. Methods Programs Biomed.* **79,** 241–257 (2005).
41. Eichelbaum, M., Kothe, K.W., Hoffman, F. & von Unruh, G.E. Kinetics and metabolism of carbamazepine during combined antiepileptic drug therapy. *Clin. Pharmacol. Ther.* **26,** 366–371 (1979).
42. Yang, J., Rostami-Hodjegan, A. & Tucker, G.T. Prediction of ketoconazole interaction with midazolam, alprazolam and triazolam: incorporating population variability. *Br. J. Clin. Pharmacol.* **51,** 472–473 (2001).
43. Gordi, T., Xie, R., Huong, N.V., Huong, D.X., Karlsson, M.O. & Ashton, M. A semiphysiological pharmacokinetic model for artemisinin in healthy subjects incorporating autoinduction of metabolism and saturable first-pass hepatic extraction. *Br. J. Clin. Pharmacol.* **59,** 189–198 (2005).
44. de Vries, J.X., Rudi, J., Walter-Sack, I. & Conradi, R. The determination of total and unbound midazolam in human plasma. A comparison of high performance liquid chromatography, gas chromatography and gas chromatography/mass spectrometry. *Biomed. Chromatogr.* **4,** 28–33 (1990).
45. Yamano, K. *et al.* Prediction of midazolam-CYP3A inhibitors interaction in the human liver from *in vivo/in vitro* absorption, distribution, and metabolism data. *Drug Metab. Dispos.* **29,** 443–452 (2001).
46. Boker, K.H., Franzen, A., Wrobel, M., Bahr, M.J., Tietge, U. & Manns, M.P. Regulation of hepatic blood flow in patients with liver cirrhosis and after liver transplantation. *Pathophysiology* **6,** 251–260 (2000).
47. Lelo, A., Birkett, D.J., Robson, R.A. & Miners, J.O. Comparative pharmacokinetics of caffeine and its primary demethylated metabolites paraxanthine, theobromine and theophylline in man. *Br. J. Clin. Pharmacol.* **22,** 177–182 (1986).
48. Lelo, A., Miners, J.O., Robson, R.A. & Birkett, D.J. Quantitative assessment of caffeine partial clearances in man. *Br. J. Clin. Pharmacol.* **22,** 183–186 (1986).
49. Soy, D., Beal, S.L. & Sheiner, L.B. Population one-compartment pharmacokinetic analysis with missing dosage data. *Clin. Pharmacol. Ther.* **76,** 441–451 (2004).